From model to visibility (Correction)

Florentin Millour [a], Gilles Duvert [b]

[a] *Max-Planck-Institut für Radio-astronomie, Auf dem Hügel 69, 53121 Bonn, Germany*

[b] *Laboratoire d'Astrophysique, Observatoire de Grenoble, 414, Rue de la Piscine, Domaine Universitaire, 38400 Saint-Martin d'Hères*

Abstract

In this paper, we carried out the previous exercises using `ASPRO` (and an image processing software for superposition of the graphs: `GIMP`) to give an idea of what one should get with `ASPRO` when following the previous exercises. **Please try to do the exercises yourself before reading these corrections**.

Key words: Optical long baseline interferometry, visibility, phase, *UV* coverage, VLTI, `ASPRO`

<u>*Exercise 1:*</u> *The diameter of a star.*

Plotting a uniform disk visibility curve: The figure produced by `ASPRO` should look like Fig. 1, left.

Zero visibility: The visibility for a uniform disk of diameter a is given by the following expression:

$$V(\rho) = 2\frac{\mathrm{J}_1(\pi a \rho)}{\pi a \rho} \tag{1}$$

$\rho = B/\lambda$ (B and λ in meters) being the spatial frequency, a being the star diameter (in radians), and J_1 the 1^{st} order Bessel function. Therefore, the value for which the visibility becomes zero is $B = 1.22\lambda/a$.

Here, the visibility zeroes around the 280 m baseline. This gives an approximately 1.89 mas diameter for the star, close to the 2 mas input.

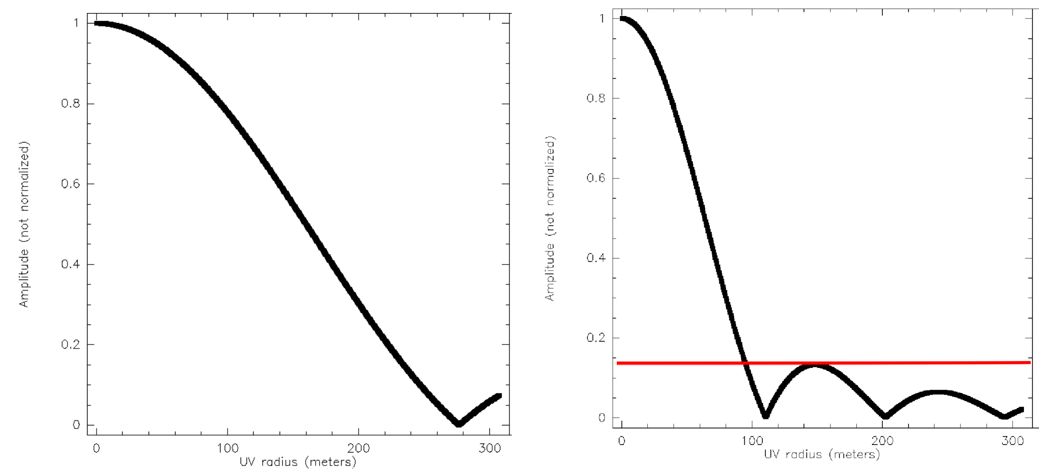

Fig. 1. **Left:** The uniform disk visibility function cut from exercise 1. **Right:** The place where one can infer a unique diameter from a single visibility measurement for a uniform disk is where the measured contrast is above 0.15. Indeed, below 0.15, several diameters can be inferred from this single visibility measurement (as shown by the red line).

Diameter uniqueness: The right plot in Fig. 1 gives a hint of the answer: There are parts of the visibility function which are monotonic (above the red line). In these parts, one visibility gives a unique solution to the diameter of the star. In the parts below the red line, a given visibility corresponds to many different solutions (as the line crosses several points of the curve). Therefore, there is a lower limit on the visibility value ($V \gtrsim 0.15$) where one can infer a unique diameter from a unique measurement.

Exercise 2: Binary.

Plotting a binary star visibility curve: The visibility and phase functions of a binary star are periodic since the image is made of Dirac functions. One can see what can be expected for a 4 mas-separation binary star in Fig. 2. One can see that the visibility does not have a cosine shape, but has sharp changes at visibility 0 for a 1 to 1 binary (black line).

Varying the flux ratio : For other flux ratios (0.8 in red, 0.5 in blue, and 0.1 in green), both the phase and visibility get smoother, and the contrast of the variations gets dimmer. Please note that these are visibility plots made with “AMP” and not “AMP$\hat{2}$” in `ASPRO`.

Phase versus visibility: To see how visibility or phase can constrain a binary star model, one can just try to change the baseline orientation and see

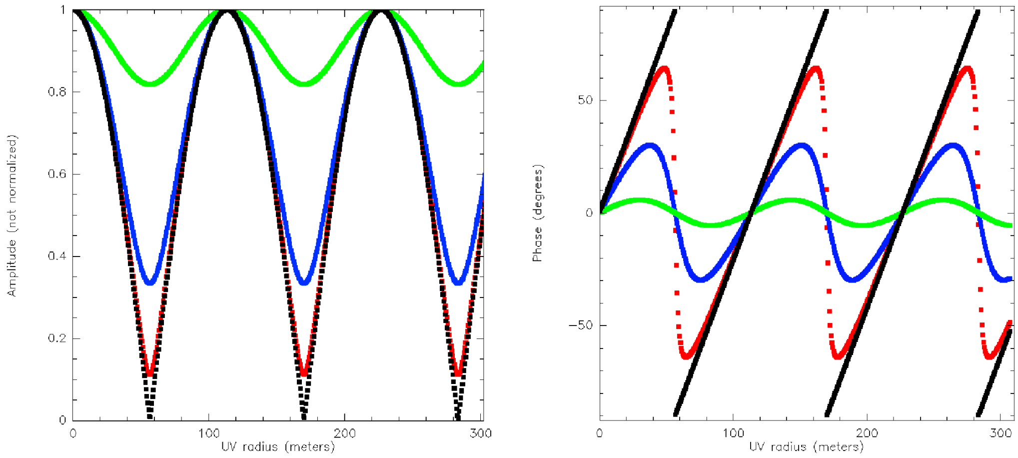

Fig. 2. **Left:** The visibility amplitude for a separation of 4 mas and different flux ratios (from the lower to the upper curves: 1 to 1 in black, 0.8 to 1 in red, 0.5 to 1 in blue, and 0.1 to 1 in green). **Right:** The visibility phase for the same separation and flux ratios.

how visibility and phase vary. In Fig. 3, bottom-right, one can see the result of such exercise. One has seen that the phase is sensitive to the contrast of the binary (Fig. 2), as is the visibility, but it is also sensitive to the position angle (both of the binary star and of the baseline) and the binary separation. Therefore, the phase can be used instead of the visibility to constrain the binary parameters!

Exercise 3: Circumstellar disk.

Plotting a Gaussian disk visibility curve: The example of this exercise is a disk of 2x4 mas and a position angle of 60 degrees. The resulting *UV* map and cuts in the *UV* plane are shown in Fig. 4.

Asphericity and visibility variations: As one can see, for a given baseline and a varying position angle, the visibility goes up and down, the minimum corresponding to the major axis and the maximum corresponding to the minor axis. One has to note (and can check) that the phase function for such a model is zero.

Exercise 4: Model confusion and accuracy.

Plotting several model visibilities: In Fig. 5 different plots are superimposed using the `GIMP` software. The uniform disk is in black, the Gaussian in

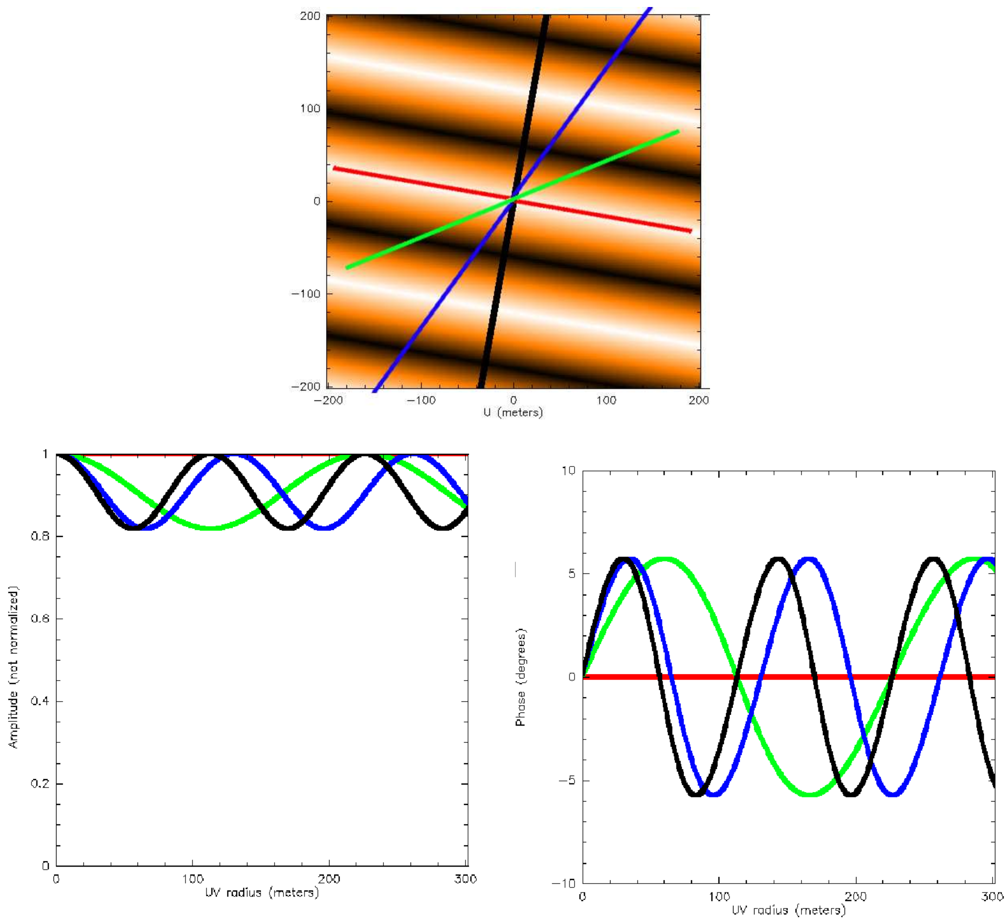

Fig. 3. **Top:** UV map showing the previous binary star visibility modulus. This visibility shows characteristic modulation stripes perpendicular to the binary orientation. **Bottom-Left:** Visibility modulus as a function of base length for the different projected stripes, in different colors (the number of sine arches increases with the different orientations): red is 90° relative to the binary orientation, green is 60°, blue is 30° and black is 0°. **Bottom-right:** Visibility phase as a function of base length for the same stripes as before.

blue, and the binary in red.

Model confusion at small baselines: Two green lines represent the 100 m and 200 m baselines. One can see the importance of multi-measurements at different baselines to be able to disentangle the different objects' shapes. With only one visibility measurement, one will never be able to distinguish between these different models. With the two visibility measurements, one can see that it will be possible to disentangle the different models if both very different baselines AND a sufficient accuracy can be reached.

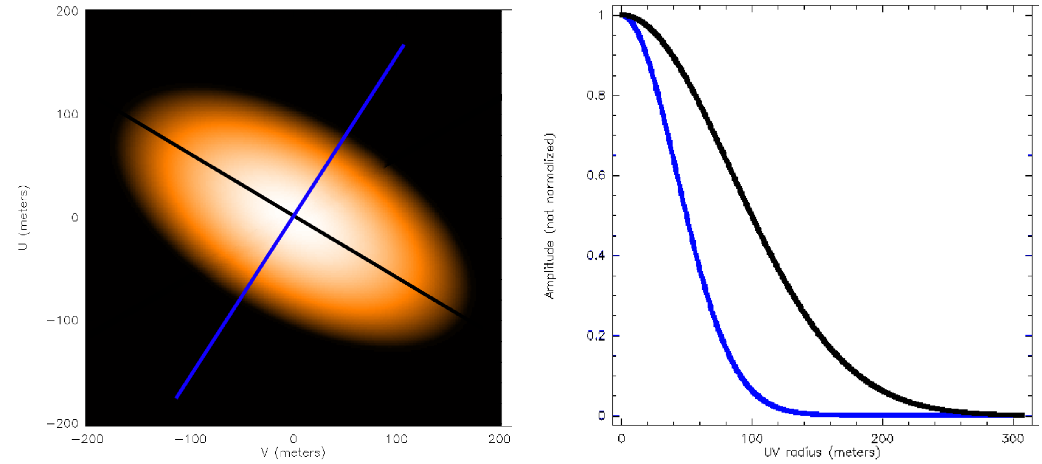

Fig. 4. **Left:** UV map showing the visibility amplitude for a 2x4 mas elongated Gaussian disk. The black and blue lines correspond to the right part of the figure. **Right:** Visibility versus base length for the minor (black, upper curve) and major (blue, lower curve) axes of the Gaussian disk. Please note that the visibility is lower in the direction of the major axis and greater in the minor axis direction.

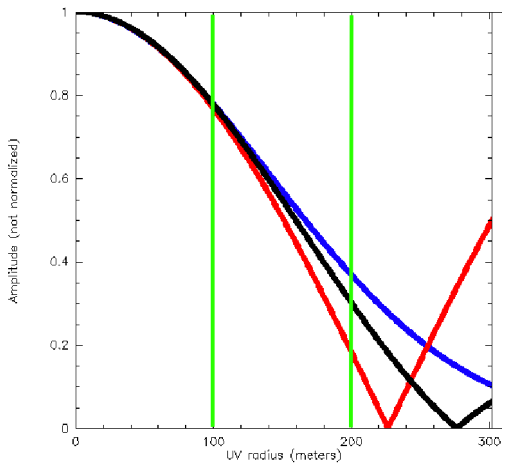

Fig. 5. Illustration of model confusion for different baselines and models: blue (top curve) is a Gaussian disk, red (bottom curve) is a binary star, and black (middle curve) is a uniform disk. The first green vertical line represents a 100 m baseline. If the accuracy is not better than about 0.01, then no distinction can be made between the different models. For the 200 m baseline (second green vertical line), an accuracy of 0.1 or better is sufficient to discriminate between the different models. Note, however, that one needs more than 1 point to be able to really distinguish between the models.

The role of measurement accuracy: Here, if one has visibility error bars of 0.05, one can distinguish between the sources using the 100 and 200 m baselines, but not with an accuracy of 0.3. This importance of accuracy in model confusion is illustrated by Fig. 6. The 1st plot (on the left) is a central point with 90% of the total flux contribution and a large (15mas) Gaussian disk around, accounting for 10% of the flux. Errors bars of 0.1 would prevent one from finding the Gaussian component, and the measured visibility (0.9 ± 0.1) would be compatible with a completely unresolved star. The right graph shows the same but with the flux ratio inverted (90% of the flux to the disk and 10% to the central star). In this case, the visibilities would be compatible with a fully resolved, extended component, given an accuracy of 0.1 on the visibility, and the point source (the central star) would not be detected. So, not only the number of baselines but also the accuracy of the measurement is of high importance to distinguish between different models.

Which baseline for which purpose: Here, one can see that since there is an unresolved source in the object image (a central source), measuring the visibility at long baseline directly provides the $\text{unresolved}_{\text{flux}}/\text{resolved}_{\text{flux}}$ flux ratio.

If one wants to get information on the disk itself (size, shape, etc.), the shorter baselines are more appropriate, since the visibility will vary according to the source shape.

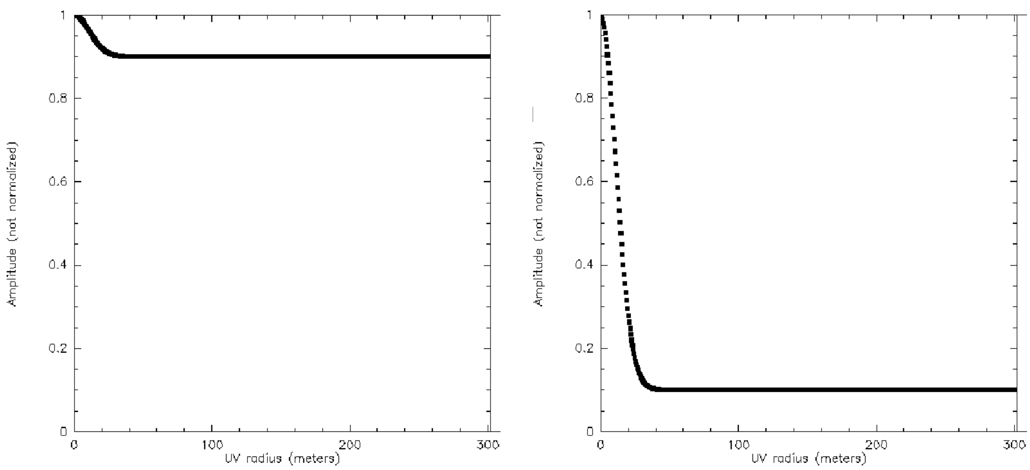

Fig. 6. **Left:** Visibility cut for a point star accounting for 90% of the total flux and a 15 mas Gaussian disk accounting for 10% of the flux. **Right:** Visibility cut for a point star accounting for 10% of the total flux and a 15 mas Gaussian disk accounting for 90% of the flux.

<u>*Exercise 5:*</u> *Choosing the right baselines.*

The idea here is to use the nice feature of `ASPRO` that is able to plot the derivatives of visibility versus the different parameters of the input model. To do so, one has to go to the *UV explore* panel, select U as X data and V as Y data, and finally select $d(AMP)/d(4)$ in the *Plot what...* part. This will plot the derivative of the visibility amplitude versus the 4^{th} parameter (radius, as shown in Table **??**).

Fig. 7 shows the model visibility and its derivative, relative to the model size, for a Gaussian disk and a uniform disk.

Uniform disk: The size used is 2 mas. The derivative peaks where the visibility slope versus baseline is the largest. This means that for a small baseline change, a large visibility change will be observed; i.e., the biggest constraint will be applied to the corresponding model in the model fitting process.

One can see that the optimal baseline is 100 m for the uniform disk. One should know that the optimal baseline to constrain a given model corresponds to a visibility of about 50%. Very important to know: baselines that are too short or too long will not reveal much information about the source size or shape.

Gaussian disk: The size used is the same as before: 2 mas. The optimal baseline is about 50 m for the Gaussian disk. Therefore, using different baselines, one will be able to both disentangle the model shape (Sharp - UD - or smooth - Gauss - edges?) and constrain the typical size (as seen before).

Exercise 6: An unknown astrophysical object.

Loading and displaying a home-made model: Fig. 8 (top) shows the model of a young stellar disk produced by F. Malbet. The star-to-disk contrast here is 1 to 10.

Please note that, as for the previous disk model (Exercise 3), the disk is elongated, and therefore, the large visibilities will correspond to the minor axis of the model, whereas the low visibilities will correspond to the major axis.

Computing the visibilities of a home-made model: The lower-left part of Fig. 8 displays a UV map of the model shown in the upper part. This map is very similar to the one shown in Fig. 4, which indicates that the disk mostly looks like a Gaussian disk.

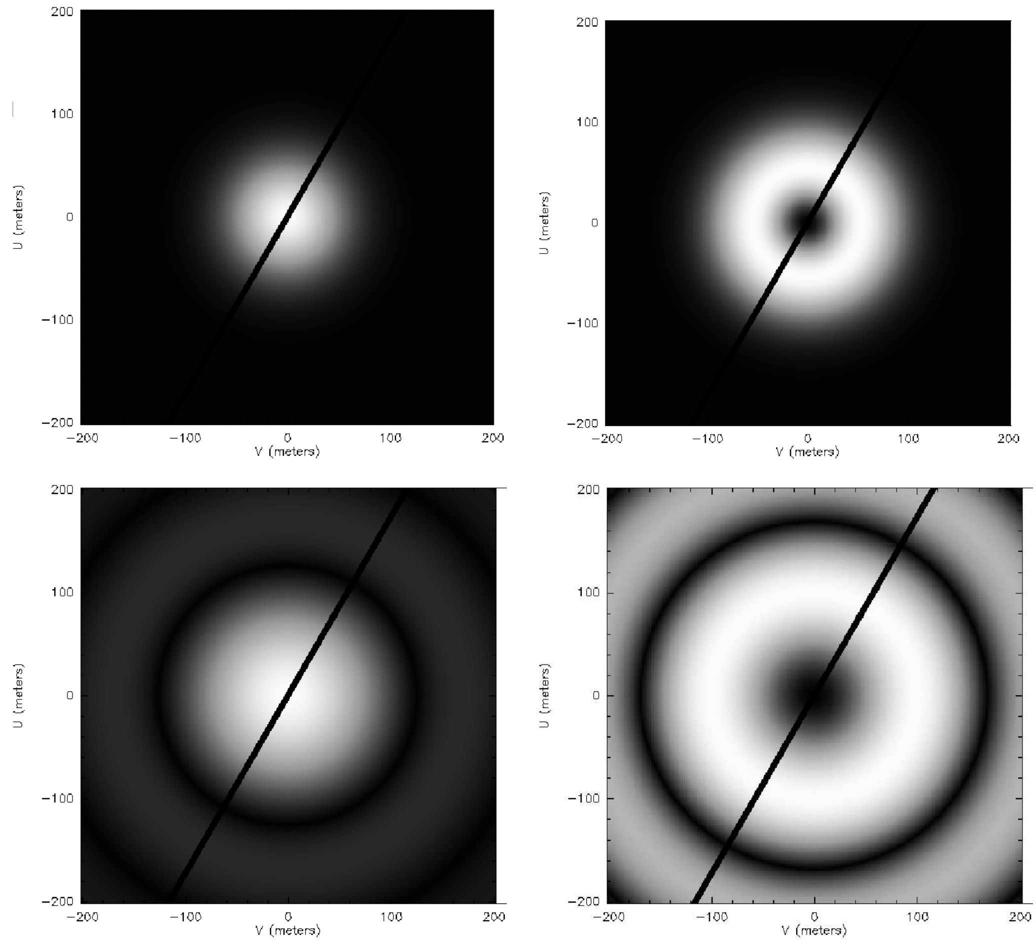

Fig. 7. **Top-left:** Gaussian disk visibility map, as a function of UV coordinates. **Top-right:** Visibility derivative versus the model size (FWHM), showing where the visibility varies more with UV coordinates. **Bottom-left:** Visibility map, but using a uniform disk. **Bottom-right:** Visibility derivative versus model size (FWHM) for a uniform disk model.

Comparing visibilities for different wavelengths: The lower-right part of Fig. 8 shows the visibility for the minor axis with different wavelengths: J (black, lower curve), K (blue, middle curve), and N (red, upper curve). This shows which wavelength to use to observe the object: the K-band allows both high visibilities for the extended component and low visibilities for the detailed structure of the disk, in the range of the VLTI offered baselines (16-130 m).

Exercise 7: Play with spectral variations, closure phases, etc.

This is a bonus exercise. To manage it, one will need the newest local version of `ASPRO` to cope with closure phases (at the time of writing this correction, the web version of `ASPRO` did not have all functionalities necessary to do this

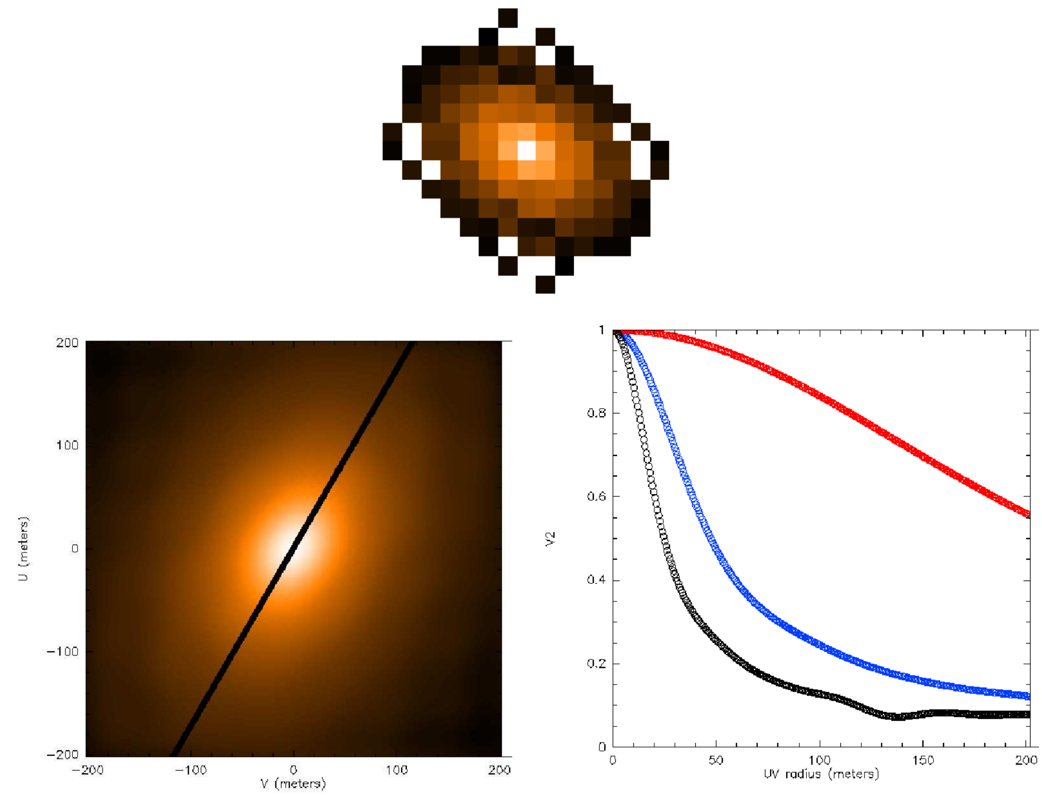

Fig. 8. **Top:** Image of the disk model used in exercise 6 (shown using the fv tool) **Bottom-Left:** Visibility map showing the main elongation of the disk, perpendicular to the main elongation of the visibility function. **Bottom-Right:** Visibility of the disk for different wavelength regimes: red (top curve) is N-band, blue (middle curve) is K-band, and black (bottom curve) is J-band.

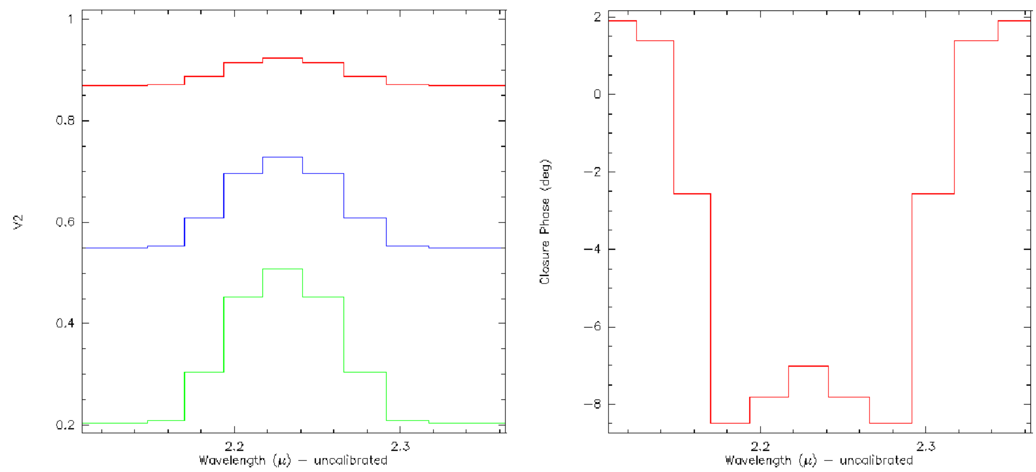

Fig. 9. **Left:** Visibility plot as a function of wavelength for different baselines (in red, green and blue). The global geometry of the model does not change, only the flux ratios between the 3 components. **Right:** Closure phase plot as a function of wavelength.

exercise). Therefore, one is not obliged to reach this point.

Plotting visibilities and closure phase versus wavelength: In Fig. 9, one can see the visibilities for a given observational setup (A0-D0-H0) and the closure phase. The author has used, on purpose, an array with aligned baselines to illustrate this exercise.

Qualitative understanding: There are a number of indicative clues to qualitatively understand the shape of the observed object:

- The different visibilities are decreasing with baseline. Therefore, the object is barely resolved by the interferometer. One cannot qualitatively distinguish between a uniform disk, a Gaussian disk, or a binary star, but one can say the object is resolved at the largest baseline (≈130m) and therefore has a size of about 2mas.
- The non-zero closure phase gives information about the asymmetry of the object. Here, one has a non-zero but very small closure phase. The only simple model known from this practice session which gives a non-zero closure phase is a binary star model. The fact that the closure phase is not 180 degrees gives the additional information that the flux ratio is not 1/1.

Therefore, only qualitatively looking at these data one can say:

- The object is likely to be a binary star,
- the separation is about 2mas,
- the flux ratio is not 1/1,
- so far, one cannot say if each component has been resolved or if there is a third component.

Looking at the solution: Fig. 10 shows the image of the model used in this exercise. As one can see, the components are somewhat resolved, but probably not enough to be detected, and a third component is present. Therefore, the qualitative analysis is not enough, and one has to perform a quantitative analysis to characterize all of these components.

References

Berger, J. P. & Segransan, D. An introduction to visibility modeling, New Astronomy Review, 2007, 51, 576-582

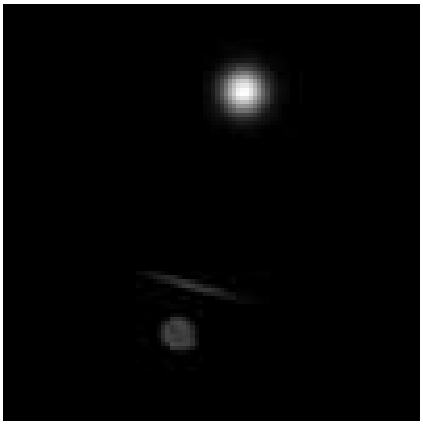

Fig. 10. Image of the binary+wind-wind collision zone model used in this exercise.

Millour, F., All you ever wanted to know about optical long baseline stellar interferometry, but were too shy to ask your adviser, New Astronomy Review, this issue.